

RR

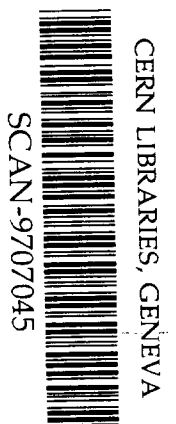


GSI-Preprint-97-31  
Juni 1997

**DECAY PROPERTIES OF GROUND-STATE AND  
ISOMER OF  $^{103}\text{In}$**

J.Szerypo, R. Grzywacz, Z. Janas, M. Karny, M. Pfützner, A. Plochocki,  
K. Rykaczewski, J. Zylicz, M. Huyse, G. Reusen, J. Schwarzenberg, P. Van Duppen,  
A. Woehr, H. Keller, R. Kirchner, O. Klepper, A. Piechaczek, E. Roeckl, K. Schmidt,  
L. Batist, A. Bykov, V. Wittman, B.A. Brown

(Accepted for publication in Z. Phys. A)



Gesellschaft für Schwerionenforschung mbH  
Planckstraße 1 • D-64291 Darmstadt • Germany  
Postfach 11 05 52 • D-64220 Darmstadt • Germany

## Decay properties of ground-state and isomer of $^{103}\text{In}$

J. Szerypo<sup>a,b</sup>, R. Grzywacz<sup>a</sup>, Z. Janas<sup>a</sup>, M. Karny<sup>a</sup>, M. Pfützner<sup>a</sup>, A. Plochocki<sup>a</sup>,  
K. Rykaczewski<sup>a,b,1</sup>, J. Żylicz<sup>a</sup>, M. Huyse<sup>b</sup>, G. Reusen<sup>b</sup>, J. Schwarzenberg<sup>b,2</sup>,  
P. Van Duppen<sup>b</sup>, A. Woehr<sup>b</sup>, H. Keller<sup>c</sup>, R. Kirchner<sup>c</sup>, O. Klepper<sup>c</sup>, A. Piechaczek<sup>c</sup>,  
E. Roeckl<sup>c</sup>, K. Schmidt<sup>c</sup>, L. Batist<sup>d</sup>, A. Bykov<sup>d</sup>, V. Wittman<sup>d</sup>, B. A. Brown<sup>e</sup>

<sup>a</sup> *Institute of Experimental Physics, Warsaw University, PL-00681 Warsaw, Poland*

<sup>b</sup> *Instituut voor Kern- en Stralingsfysica, University of Leuven, B-3001 Leuven, Belgium*

<sup>c</sup> *Gesellschaft für Schwerionenforschung, D-64220 Darmstadt, Germany*

<sup>d</sup> *St. Petersburg Nuclear Physics Institute, 188-350 Gatchina, Russia*

<sup>e</sup> *NSCL, Department of Physics and Astronomy, MSU, East Lansing,  
MI 48824-1321, USA*

June 4, 1997

**Abstract.** The  $\beta$ -decay properties of ground-state and isomer of  $^{103}\text{In}$  were investigated by means of  $\gamma$ -ray spectroscopy. The half-lives of  $^{103g}\text{In}$  and  $^{103m}\text{In}$  were determined to be  $60 \pm 1$  s and  $34 \pm 2$  s, respectively. Out of 149  $\gamma$  transitions ascribed to the decay of  $^{103g}\text{In}$ , 104 have been placed in a decay scheme including 55 excited states of  $^{103g}\text{Cd}$ . The main part of the resulting distribution of the Gamow-Teller strength  $B(\text{GT})$  is associated with the feeding of  $^{103}\text{Cd}$  levels at excitation energies around 3 MeV. This observation can be interpreted as a sign of dominant feeding of three-quasiparticle states in  $^{103}\text{Cd}$ , which correspond to the  $1^+(\pi g_{9/2}^{-1}, \nu g_{7/2}) \otimes \pi g_{9/2}$  shell-model configuration spread over many levels. The sum of the  $B(\text{GT})$  values deduced from the present  $\gamma$ -ray data amounts to 0.34, which provides a lower limit to the total Gamow-Teller strength. The  $B(\text{GT})$  distribution for  $^{103}\text{In}$  decay is compared to the corresponding experimental results for  $^{105,107,109}\text{In}$  and to theoretical predictions for  $^{99,101}\text{In}$ . The latter were calculated by using an advanced spherical shell model. The  $\beta$ -branching ratio for the  $^{103m}\text{In}$  decay is estimated and compared with the relevant values for the neighbouring indium isotopes including  $^{101}\text{In}$  whose half-life was determined to be  $14.9 \pm 1.2$  s.

**Keywords:** RADIOACTIVITY  $^{103}\text{In}$  (EC), ( $\beta^+$ ) [from  $^{50}\text{Cr}(^{58}\text{Ni}, 3p2n)$ ,  $E = 5.9$  MeV/nucleon]; Measured  $E_\gamma$ ,  $I_\gamma$ ,  $\gamma\gamma$ -coin,  $T_{1/2}$ .  $^{103}\text{Cd}$  deduced levels, Gamow-Teller strength distribution. Ge detectors, on-line mass separation.

**PACS:** 21.10.-k; 21.60.Cs; 23.40.Hc; 27.60.+j

---

<sup>1</sup>Present address: Oak Ridge National Laboratory, Physics Division, PO Box 2008, Oak Ridge, Tennessee 37831-6371, USA

<sup>2</sup>Present address: Nuclear Structure Laboratory, University of Notre Dame, Notre Dame, Indiana 46556, USA

# 1 Introduction

The ground-state of odd- $A$  indium isotopes in the vicinity of doubly-magic  $^{100}\text{Sn}$  is expected to have spin and parity  $I^\pi = 9/2^+$  due to the coupling of an unpaired  $g_{9/2}$  proton to the cadmium even-even core. Since there are nine  $g_{9/2}$  protons available for the Gamow-Teller (GT) transformation  $\pi g_{9/2} \rightarrow \nu g_{7/2}$ , the  $\beta$ -decay is expected to be fast. Within the Elementary Single Particle Shell Model (ESPSM), two GT decay modes are expected for odd- $A$  neutron-deficient indium isotopes, namely: (i) a transformation of an unpaired (odd)  $g_{9/2}$  proton into a  $g_{7/2}$  neutron, and (ii) a transformation of a  $g_{9/2}$  core proton into a  $g_{7/2}$  neutron. The latter disintegration mode leads to the GT pair ( $\pi g_{9/2}^{-1}, \nu g_{7/2}$ ) coupled to spin and parity  $1^+$ , and leaves the odd proton as a spectator. An account for the pairing interaction in the daughter nucleus (ESPSM+BCS) would correspond to a replacement of single-particle and three-particle states by one-quasiparticle ( $1qp$ ) and three-quasiparticle ( $3qp$ ) states at excitation energies of a few hundred keV and about 3 MeV, respectively. The interpretation of the GT-strength distribution  $B(\text{GT})$  and, in particular, the ratio between the  $B(\text{GT})$  values of the two expected decay modes, should allow for a better understanding of the GT quenching phenomenon, complementing the data obtained for the simpler but decay-energy limited decays of even-even nuclei in the  $^{100}\text{Sn}$  region [1].

Another important nuclear structure information can be gained for odd- $A$  indium from M4 isomers, lying at excitation energies of about 600–700 keV. These M4 proton-hole isomers, with spin and parity  $I^\pi = 1/2^-$ , are formed by promoting one of the core  $p_{1/2}$  protons into the  $g_{9/2}$  orbital. The excitation energy of such isomers is directly related to the energy gap between  $p_{1/2}$  and  $g_{9/2}$  proton orbitals, and thus allows to study the gap evolution with increasing neutron number. One should note that such states are, due to their comparatively low spin values, hardly accessible by using in-beam techniques, while they might be identified and studied by means of decay spectroscopy, in particular at an on-line mass separator.

For very neutron-deficient odd-mass indium isotopes, the  $\beta$ -decay of the  $1/2^-$  isomer can compete with the M4 deexcitation. Decay studies of both ground-state and isomer would give a direct comparison between the GT transformation of the even-even core plus a single  $g_{9/2}$  proton (the ground state) and that of the even-even core alone (the isomer).

For such complex decays the total absorption spectrometer (TAS) [2] is a suitable spectroscopic tool, as the GT-strength is spread over many highly excited daughter states, which results in statistical  $\gamma$ -ray cascades and hence in difficulties of establishing the true  $\beta$ -feeding pattern. However, without the information on the discrete part of the decay scheme, the deconvolution of TAS spectra is unreliable.

Extensive spectroscopic data exist on the decay properties of odd- $A$  indium isotopes with  $A \geq 105$ . These results do not yield any evidence for  $\beta$ -decay of the  $1/2^-$  isomers. However, for lighter indium isotopes the data are very limited. In case of the  $^{103g}\text{In}$  only a partial decay scheme is known [3]. For the  $^{103m}\text{In}$ , preliminary data on half-life and isomeric energy were obtained, and the intensity for the possible  $\beta$ -decay branching was estimated [4]. The data on  $^{101}\text{In}$  are even more scarce [5].

Based on the arguments presented so far, we decided to reinvestigate, by means of the high-resolution  $\gamma$ -ray spectroscopy, the decay properties of the ground-state and the  $1/2^-$  isomer of  $^{103}\text{In}$  and  $^{101}\text{In}$ . From earlier studies of odd-odd indium isotopes (see e.g. [6]), the main GT strength was expected to stem from the decay of the even-even core. As

mentioned above, this may lead to difficulties in resolving and detecting the (statistical)  $\gamma$ -rays emitted from high-lying levels in the daughter nucleus. However, in case of the decay of odd-even indium isotopes the excitation energy of these levels is expected to be about 2–3 MeV lower compared to the decay of odd-odd indium. Therefore, the  $\gamma$ -transitions of interest should be less closely spaced and the resulting decay scheme could thus be more complete.

## 2 Experimental procedure

The experiment was performed at the GSI on-line mass separator.  $^{103}\text{In}$  and  $^{101}\text{In}$  were produced in  $^{50}\text{Cr}(^{58}\text{Ni},3\text{p}2\text{n})$  and  $^{50}\text{Cr}(^{58}\text{Ni},3\text{p}4\text{n})$  reactions, respectively. A 5.9 MeV/u  $^{58}\text{Ni}$  beam of about 20 particle nA impinged on an enriched  $^{50}\text{Cr}$  target (3.3–4.6 mg/cm<sup>2</sup>, enrichment 91% or 97%, on 2 or 2.3 mg/cm<sup>2</sup>  $^{nat}\text{Mo}$  backing) that was mounted in front of a FEBIAD-E [7] plasma-discharge ion source. This source yielded mass-separated beam intensities of about 7100 atoms/s for  $^{103g}\text{In}$  and about 140 atoms/s for  $^{103m}\text{In}$ .

The mass-separated A=103 activities were implanted in a transport tape. After a collection time of 80 s, the sources were transported to the counting station and measured during 80 s. This station included two Ge detectors, positioned in close geometry to the source, on opposite sides of the tape. One of them was a large-volume 70% detector and the second one a high-resolution low-energy detector (LEGe). The full-energy peak efficiencies of the detectors, determined by using standard calibration sources, reached maximum values of 13% and 22% at energies of 120 and 70 keV, respectively.

The  $\gamma$ -ray singles spectra were measured in multispectrum mode with 8 time subgroups of 10 s each. Coincidence data were stored event-by-event using the GOOSY acquisition system on a VAX computer. An example of a  $\gamma$ -ray spectrum in the region of the strongest  $\gamma$ -lines of  $^{103}\text{In}$  is shown in Fig. 1.

The spectra, measured in both detectors, were distorted due to summing effects occurring with coincident  $\gamma$ -ray cascades, 511 keV quanta, positrons and/or X-rays. Since the latter kind of summing was suppressed in the large-volume detector due to its thick entrance window, the photopeak intensities determined by means of this detector were chosen to be corrected for summing with  $\gamma$  and 511 keV quanta and to thus yield the correct photopeak areas. For this purpose a FORTRAN program was written [8], based on the formalism presented in [9, 10, 11]. The summing calculations were performed with the following approximations:

- The photopeak-to-total efficiency ratio was measured not for the  $\gamma$ -detector used in this experiment, but for another, very similar one which had also a relative efficiency of 70%.
- Due to lack of an annihilator around the source position, the efficiency for 511 keV annihilation radiation was not well defined. In order to estimate this efficiency, the peak areas for some stronger  $\gamma$ -lines, arising from summation with annihilation radiation, were calculated with the computer program. Subsequently, the efficiency for 511 keV  $\gamma$ -rays was adjusted so that the calculated peak areas matched the measured ones. The resulting efficiency was by a factor of 2.5 lower than that obtained by using standard  $\gamma$ -ray sources.
- Summation due to positrons entering the detector was not accounted for.

It was checked that, in case of the  $^{103}\text{In}$  decay scheme presented in this paper, the influence of the first two approximations on the final  $\gamma$ -intensities is relatively small. This is probably due to the fact that the  $^{103}\text{In}$  decay populates many final levels with intensities that are not drastically (by more than one order of magnitude) different. However, these approximations might have a large influence on the photopeak areas calculated by using the computer program. Therefore, the absolute intensities derived for mass-separated beams of  $^{103g}\text{In}$  and  $^{103m}\text{In}$  should be considered to have uncertainties of about 50% and 10%, respectively.

## 3 Experimental results

### 3.1 $\beta$ -decay of $^{103g}\text{In}$

Prior to our work, 13  $\gamma$ -lines were assigned to the decay of  $^{103}\text{In}$  [3]. Due to missing coincidence relations, only the seven strongest transitions were tentatively placed in a level scheme, this procedure being based on the systematic trend emerging from neighbouring isotopes and isotones.

Our measurements allowed us to identify, from a detailed analysis of  $\gamma$ -singles and  $\gamma\gamma$ -coincidence data, 149  $\gamma$ -rays as being due to the  $\beta^+$ /EC-decay of  $^{103g}\text{In}$ . A list of the corresponding  $\gamma$ -ray energies and intensities, together with information on the  $\gamma\gamma$ -coincidence relationships, are presented in Table 1. These data were obtained during a measurement time of 10 h. The assignment of  $\gamma$ -lines to the  $^{103g}\text{In}$  decay was established by a comparison of experimental half-lives. An additional criterion was the observation of coincidence relations with cadmium KX-rays and/or with more intense  $\gamma$ -rays that were already assigned on the basis of their half-life. The weighted average of the  $^{103g}\text{In}$  half-life, obtained from the multispectrum analysis for the 24 most intense lines, is  $60 \pm 1$  s. This result is in agreement with the previously obtained values of  $64.8 \pm 6.6$  s [12] and  $70.8 \pm 6.0$  s [3], with a  $1.6\sigma$  deviation in the latter case.

Five  $\gamma$ -rays assigned by Verplancke et al. [3] to the  $^{103g}\text{In}$  decay are not confirmed by our analysis. We found these lines to be too weak for even a tentative assignment, and hence did not include them in Table 1. On the one hand, Verplancke et al. reported  $\gamma$ -transitions of 595.53(37), 609.12(34) and 1778.66(13) keV with intensities, relative to that of the 187.9 keV line, of 6.1(1), 6.1(1) and 9.1(41)%, respectively. Our data yield only upper limits of 0.1% for these  $\gamma$ -rays. In the case of the 609.1 keV line, we took contributions from transitions at 609.3 keV ( $^{214}\text{Bi}$  from room background) and 608.6 keV ( $^{103g}\text{Ag}$  as isobaric beam contaminant) into account. On the other hand, we found  $\gamma$ -rays of 315.3 keV and 640.6 keV, given in [3] with intensities of 2.7(9) and 4.7(36)%, respectively, to be an order of magnitude weaker. The 640.6 keV line is dominated by the 640.8 keV  $\gamma$ -ray of  $^{103}\text{Cd}$ , which has been corrected for in our analysis.

Fig. 2 shows the decay scheme of  $^{103g}\text{In}$  which accounts for 104 out of 149 transitions, i.e. for 93% of the observed  $\gamma$ -ray intensity (see Table 1). Transitions and levels marked in Fig. 2 by dashed lines have been placed tentatively in the decay scheme. The normalization of transition intensities was achieved by assuming that the  $5/2^+$   $^{103}\text{Cd}$  ground-state is not fed directly in the  $^{103g}\text{In}$  decay, and that the total intensity of  $\gamma$ -rays leading to this state amounts to 100%. Corrections for internal conversion have been taken into account for the 187.9, 202.0 and 719.9 keV transitions, assuming their multipolarities to be M1,

E2 and E2, respectively. Multipolarities as well as spins and parities of the relevant levels were taken from [3]. In a few cases the  $\gamma$ -lines were identified as multiplets. The exact energies and intensities of the multiplet members were derived either from a multicomponent fit to these lines in the singles  $\gamma$ -ray spectrum, or estimated from the coincidence spectra.

In comparison to the previous data [3], our decay scheme excludes the level at 367.5 keV and places the corresponding transition as populating the 202.0 keV level. Moreover, the 916.7 keV transition was found not to be a ground-state transition from the corresponding level, but to feed the 187.9 keV level. Our data agree with data from in-beam work [13] as far as the  $\gamma$ -transitions of 168.0, 187.9, 552.1, 604.7, 719.9, 740.4 and 772.4 keV are concerned.

### 3.2 Decay properties of the $1/2^-$ isomer in $^{103}\text{In}$

The presence of a long-lived isomer  $^{103m}\text{In}$  has already been reported in the work of Decrock [4] who identified the isomer by its internal transition (IT) and measured the isomeric energy and the half-life to be  $630.6 \pm 0.5$  keV and  $35 \pm 5$  s, respectively. Decrock used a  $^{92}\text{Mo}(^{14}\text{N},3n)$  reaction and found the isomeric yield to be 10% of that of the ground-state. Due to this rather large isomeric ratio, it was possible to observe that the half-life of cadmium KX-rays is smaller than that of  $^{103g}\text{In}$ , the latter being derived from the time analysis of  $\gamma$ -rays. The difference, which was interpreted as being due to an admixture of KX-rays from the decay of the (shorter-lived) isomeric activity to KX-rays from the ground-state decay, proves the existence of  $\beta^+$ /EC-decay of  $^{103m}\text{In}$ . (The effect presumably stems from the isomeric EC-decay itself rather than from the conversion of  $\beta$ -delayed transitions from  $^{103m}\text{In}$  decay.) The time analysis of cadmium KX-rays permitted Decrock to estimate the  $\beta$ -decay branch of  $^{103m}\text{In}$  to be 67%, leaving 33% for the IT. In the  $^{50}\text{Cr}(^{58}\text{Ni},3p2n)$  reaction, used in our experiment, the isomer ratio amounted to only 2%. This was probably the reason why we did not observe any difference in half-life between the  $\gamma$ -lines, assigned to  $^{103g}\text{In}$ , and cadmium KX-rays. The energy of the IT was determined as  $631.7 \pm 0.1$  keV. Its time analysis yielded a half-life of  $34 \pm 2$  s, as illustrated in Fig. 3.

### 3.3 $\beta$ -decay of $^{101}\text{In}$

For the  $\beta$ -decay of  $^{101}\text{In}$ , four  $\gamma$ -transitions were identified and a half-life value of  $16 \pm 3$  s was measured at the Louvain-la-Neuve on-line mass separator [5]. From our data we are able to confirm two of these  $\gamma$ -lines, namely those at 252 and 892 keV, and to show that they are in coincidence with each other. The half-life of  $^{101}\text{In}$  was redetermined with improved accuracy to be  $14.9 \pm 1.2$  s. This activity is assigned to  $^{101g}\text{In}$ , whereas we have not obtained any evidence for the existence of an isomeric state in  $^{101}\text{In}$ .

## 4 Discussion

### 4.1 Gamow-Teller strength

On the basis of the  $^{103}\text{In}$  decay scheme displayed in Fig. 2, a  $\gamma$ -intensity balance was performed for each level, ascribing the difference between the  $\gamma$ -intensity depopulating and

populating a given level to its  $\beta$ -feeding. This standard technique of decay spectroscopy has the disadvantage that for large decay  $Q$ -values only an *upper limit* for the  $\beta$ -feeding of the selected level can be obtained, as numerous unobserved (weak)  $\gamma$ -rays may populate this level (see also the discussion of this problem for the case of  $^{104}\text{In}$  [6]). Therefore, both the  $\gamma$ -intensities, listed in Table 1, and the  $\beta$ -feeding values, derived from  $\gamma$ -intensity balance, have unknown systematical uncertainties. The 50% uncertainty mentioned in Section 1 holds only for the  $\gamma$ -rays of 187.9 and 630.6 keV.

By taking the  $\beta$ -feeding results at face value and using  $Q_{EC} = 6.05 \pm 0.02$  MeV [14], we determined  $\log ft$  values and transformed them into a B(GT) distribution according to [15]

$$B(\text{GT}) = \frac{3860 \text{ s}}{ft} \quad (1)$$

The resulting B(GT) distribution is shown as a solid-line histogram in Fig. 4c. For  $^{103}\text{Cd}$  excitation energies above 0.5 MeV, where  $3qp$  states are expected (see Section 1), the B(GT) values are summed over energy intervals of 0.5 MeV. In Fig. 4c, the feeding of the  $1qp$   $7/2^+$  state below 0.5 MeV is shown as a single bar. The total strength  $B_{\Sigma}(\text{GT})$ , taken as the sum of the partial strengths for different energy bins, including the  $1qp$  contribution, is equal to 0.34.

The distribution displayed as a solid-line histogram in Fig. 4c ends at 4 MeV. This is due to the limited sensitivity of our detection set-up, in particular to higher-energy  $\gamma$ -rays, as well as due to the limited energy range, 0–4 MeV, of our  $\gamma$ -spectra. It is evident that our data do not include the GT-strength associated with highly excited levels of  $^{103}\text{Cd}$  and their (statistical)  $\gamma$ -ray deexcitation. To illustrate the influence of limits in  $\gamma$ -detection efficiency, we investigated those  $\gamma$ -transitions which were not placed in the decay scheme. For this purpose we assumed arbitrarily that they all feed the  $^{103}\text{Cd}$  ground-state. Under this assumption, the total strength  $B_{\Sigma}(\text{GT})$  increases to 0.43, while the B(GT) distribution changes its shape as indicated by the dashed histogram shown in Fig. 4c. The unassigned transitions, which carry about 7% of the total  $\gamma$ -ray intensity, may thus be responsible for more than a quarter of the total GT-strength.

In Figs. 4d, 4e and 4f, the B(GT) distributions for the neighbouring odd- $A$  indium isotopes  $^{105,107,109}\text{In}$  are displayed as derived from discrete  $\gamma$ -ray spectroscopy [16, 17, 18]. The experimental  $B_{\Sigma}(\text{GT})$  amount to 0.26, 0.32 and 0.25, respectively. These data strongly suggest that with increasing mass-number, i. e. decreasing  $Q_{EC}$  window, an increasing part of the GT-strength was not observed by  $\beta$ -decay measurements. The ratio  $B_{3qp}(\text{GT})/B_{1qp}(\text{GT})$  of the  $\beta$ -strengths for the two possible decay patterns, i. e. the transition to  $3qp$  (core) states in the respective daughter (cadmium) isotope relative to that to  $1qp$  levels, was derived from the experimental data (see Figs. 4c, 4d, 4e and 4f) to be 140:1, 40:1, 37:1 and 11:1 [15] for the decays of  $^{103}\text{In}$ ,  $^{105}\text{In}$ ,  $^{107}\text{In}$  and  $^{109}\text{In}$ , respectively. The ESPSM prediction for indium isotopes amounts to 44:1 [15]. As mentioned above, part of the GT-strength related to the  $3qp$  decay mode has probably been missed by the measurements. Therefore, the experimental  $B_{\Sigma}(\text{GT})$  values of  $^{103}\text{In}$  as well as those of  $^{105,107,109}\text{In}$  should be regarded as lower limits only. This conclusion is confirmed by, e. g., data obtained for the odd-even nucleus  $^{96}\text{Rh}$  ( $Q_{EC} = 5.11 \pm 0.15$  MeV) [21] and the odd-odd nucleus  $^{104}\text{In}$  ( $Q_{EC} = 7.91 \pm 0.14$  MeV) [6, 19]. In the former case, the experimental  $B_{3qp}(\text{GT})/B_{1qp}(\text{GT})$  value, deduced from high-resolution  $\gamma$ -ray measurements, is 30:1 whereas the ESPSM result is 7.33:1 [15]. In the latter case, the ratio of  $\beta$ -strengths for transitions to  $4qp$  (core) and  $2qp$  states was deduced from TAS data [19] to be 600:1

compared to the ESPSM value of 44:1 [15].

All in all, these data indicate the dominant role of the even–even core decay, in particular for the large  $Q_{EC}$  windows of light indium isotopes. Unfortunately, calculations within the large model space of the advanced spherical shell model (ASSM), performed by Brown and Rykaczewski [20], are not yet possible for  $^{103}\text{In}$  and heavier indium isotopes. It is clear from the above discussion that model calculations for the GT–decay, that go beyond ESPSM, are needed for these nuclei.

The GT–quenching factor, i.e. the ratio between the  $B(\text{GT})$  value obtained from the ASSM calculation and the corresponding experimental result, was found [20] to be 3.8 for the decay of even–even nuclei near  $^{100}\text{Sn}$ . This result was based on experimental data for the decay of  $^{98}\text{Cd}$  ( $N=50$ ). Correspondingly, we used data measured for the decay of  $^{95g}\text{Rh}$  ( $N=50$ ) [21] to estimate a GT–quenching factor of 7.0 for odd–even nuclei near  $^{100}\text{Sn}$ . This factor was taken into account in the ASSM calculation of the  $B(\text{GT})$  values displayed in Figs. 4a and 4b as well as the  $B_{\Sigma}(\text{GT})$  and half–life values listed in Table 2. The half–lives of  $^{99g}\text{In}$  and  $^{101g}\text{In}$  are predicted to be 2.1 s and 13 s, respectively. The latter value agrees with the experimental result of  $4.9 \pm 1.2$  s. The  $\beta$ –decay of the  $1/2^-$  isomers will be further discussed in Section 4.2.

## 4.2 M4 isomerism in odd–A indium isotopes

A priori, the  $1/2^-$  isomer in odd–A indium isotopes may decay either via an M4 IT to the ground–state, or via  $\beta$ –decay to excited states in the cadmium daughter. These M4 decay rates are hindered by about a factor of 6 compared to the ASSM calculations. It was already noticed earlier [3] that the experimental half–lives of  $1/2^-$  isomers for  $A \geq 105$  agree well with estimates obtained for single–proton transitions [22]. This confirms the relatively pure single–particle character of the isomeric state. We make use of this observation in order to deduce the decay characteristics of the isomers, in particular their  $\beta$ –decay branching ratio. As can be seen from Figs. 4a and 4b as well as from Table 2, ASSM predicts that the  $\beta$ –decay of the  $1/2^-$  isomer of  $^{99}\text{In}$  and  $^{101}\text{In}$  carries even more GT–strength than that of the respective ground–state. This is due to the fact that, within the framework of ASSM, one of the  $p_{1/2}$  protons is promoted to the “GT–active”  $g_{9/2}$  orbital. Therefore, one expects a sizable  $\beta$ –decay branch of the  $1/2^-$  isomers also for heavier indium isotopes.

The properties of  $^{101m-109m}\text{In}$  from measurements or semiempirical estimates are compiled in Table 3. We expect that, in case of  $\beta$ –decay occurring from both ground–state and isomer, the respective probabilities are mainly determined by the even–even core decay. Consequently, the partial half–life  $T_{1/2,\beta}$  for  $\beta$ –decay of the isomer may, to first order, be approximated by the experimental ground–state half–life  $T_{1/2,g.s.}^{exp}$  for the decay of the ground–state. This approach, which neglects for simplicity the possible half–life change stemming from the energy difference of both states, is supported by the ASSM predictions of ground–state and isomeric half–lives of  $^{99}\text{In}$  and  $^{101}\text{In}$  (see Table 3). From a comparison of  $T_{1/2,g.s.}^{exp}$  and the experimental half–life  $T_{1/2}^{exp}$  of the isomer, we conclude that in case of  $^{107m}\text{In}$  and  $^{109m}\text{In}$  the decay proceeds only via the IT, i.e.  $I_{\gamma+ce} \approx 100\%$  and  $I_{\beta} \approx 0$  for the IT and  $\beta$ –branching ratio, respectively. In order to deduce the branching ratios for lighter indium isomers, we proceed in the following way:

- For each isomeric state, we determine its Moszkowski half–life estimate  $T_{1/2,\gamma+ce}^M$  [22].



- For  $^{107m}\text{In}$  and  $^{109m}\text{In}$ , we calculate the ratio of  $T_{1/2}^{exp}$  and  $T_{1/2,\gamma+ce}^M$ . The resulting two numbers serve as scaling factors, with which the  $T_{1/2,\gamma+ce}^M$  values of  $^{105m}\text{In}$ ,  $^{103m}\text{In}$  and  $^{101m}\text{In}$  are multiplied. This procedure yields limits for the partial IT half-life ( $T_{1/2,\gamma+ce}^{scaled}$ ) of these nuclides.

- By using the formula

$$\frac{1}{T_{1/2}^{exp}} = \frac{1}{T_{1/2,\gamma+ce}^{scaled}} + \frac{1}{T_{1/2,\beta}} \quad (2)$$

we deduce limits for  $T_{1/2,\beta}$  and the branching ratios  $I_{\gamma+ce}$  and  $I_{\beta}$ .

As can be seen from Table 3, this analysis predicts that  $\beta$ -decay becomes an important disintegration mode already for  $^{105m}\text{In}$  and dominates the decay of  $^{103m}\text{In}$  and  $^{101m}\text{In}$ . One should note the good agreement of such an  $I_{\beta}$  estimate for  $^{103m}\text{In}$  with the experimental result of about 67% obtained by Decroock et al. [4].

## 5 Conclusion

We have substantially extended the decay scheme of  $^{103}\text{In}$ , which allowed us to derive a lower limit for the GT-strength for its decay. The new experimental data shows that the main part of the GT-strength is associated with feeding of  $^{103}\text{Cd}$  states at excitation energies near 3 MeV or above. This interpretation agrees with results obtained from an ESPSM+BCS model which predict the decay to occur mainly within the even-even core leading to  $3qp$  states of the  $1^+(\pi g_{9/2}^{-1}, \nu g_{7/2}) \otimes \pi g_{9/2}$  shell-model configuration. The experimental  $B_{\Sigma}(\text{GT})$  value for  $^{103}\text{In}$  is considerably lower than expected from an extrapolation of the ASSM predictions for  $^{99}\text{In}$  and  $^{101}\text{In}$ . This may partly be related to the fact that some fraction of the GT-strength is missed by experiments performed with standard high-resolution (low-efficiency) germanium detectors. The situation could be clarified by studying the  $^{103}\text{In}$  decay by means of the TAS technique.

For odd- $A$  indium isotopes with  $A \geq 103$  the energy window for  $\beta$ -delayed proton emission is small, e. g. 1.4 MeV for  $^{103}\text{In}$  [14]. Therefore, there does not seem to be much need to include this disintegration mode in GT-studies of light indium isotopes, except if experiments on  $^{101}\text{In}$  or  $^{99}\text{In}$  are envisaged.

Our work has also improved the data on  $^{103m}\text{In}$  and confirms the importance of its  $\beta$ -decay. The  $\beta$ -decay branching ratio for the yet unknown  $^{101m}\text{In}$  is estimated to be larger than 90%. Therefore, this isomer could be searched for by detecting positrons or  $\beta$ -delayed protons rather than  $\gamma$ -rays. ASSM predicts the half-life of  $^{101g}\text{In}$  to be 13 s in good agreement with the experimental result.

### Acknowledgements

The authors from Warsaw would like to kindly acknowledge the support and hospitality of GSI. This work was supported in part by the Polish Committee of Scientific Research under grant KBN 2 P03B 039 13, and by the European Community under Contracts No. ERBCIPD-CT-940091 and ERBCIPD-CT-950083. BAB acknowledges support from NSF grant PHY-94-03666.

## Figure captions:

Fig. 1. Part of the  $\gamma$ -ray spectrum measured with an implantation/decay cycle of 80/80 s. The most prominent  $\gamma$ -lines from the decay of  $^{103}\text{In}$ ,  $^{103}\text{Cd}$  and  $^{103}\text{Ag}$  are marked with "In", "Cd" and "Ag", respectively.

Fig. 2. Scheme of  $^{103}\text{Cd}$  levels fed in the decay of  $^{103}\text{In}$ . Transitions in  $^{103}\text{Cd}$  are marked by their energies (in keV) and relative intensities. Spin and parity assignments were taken from [13]. Transitions and levels marked by dashed lines were placed tentatively in the decay scheme.

Fig. 3. Determination of the  $^{103m}\text{In}$  half-life. The data points have been corrected for the dead time of the corresponding multispectrum subgroup.

Fig. 4. B(GT) distributions for the decays of  $^{99}\text{In}$  (a),  $^{101}\text{In}$  (b),  $^{103}\text{In}$  (c),  $^{105}\text{In}$  (d),  $^{107}\text{In}$  (e) and  $^{109}\text{In}$  (f). The  $Q_{EC}$  values indicated are taken from [14] for ground-state to ground-state transitions. The B(GT) values represent experimental results except for the panels (a) and (b), which show predictions obtained from shell-model calculations [20] for the decay of the ground state (solid line) and the isomer (dashed line), respectively, and include a Gamow-Teller quenching factor of 7.0 (see text for details). The height of each histogram segment corresponds to the sum of B(GT) values for an excitation-energy interval of 0.5 MeV. For excitation energies below 0.5 MeV, the height of each bar corresponds to the B(GT) value for the individual  $\beta$ -transition to the single ( $1qp$ ) level. For  $^{103}\text{In}$  (c), the "apparent" experimental B(GT) distribution based on  $\gamma$ -lines placed in the decay scheme is shown as a solid line, whereas the dashed line displays the B(GT) distribution obtained under the assumption that  $\gamma$ -lines which are not placed in the decay scheme feed the  $^{103}\text{Cd}$  ground-state.

## References

- [1] K. Rykaczewski, in *Proc. 6th Int. Conf. on Nuclei far from Stability and 9th Int. Conf. on Atomic Masses and Fundamental Constants*, Bernkastel-Kues, 1992, eds. R. Neugart and A. Wöhr, IOP Publishing (Bristol, Philadelphia), Inst. Phys. Conf. Ser. 132, Section 5 (1993) 517.
- [2] M. Karny, J. M. Nitschke, L. F. Archambault, K. Burkard, D. Cano-Ott, M. Hellström, W. Hüller, R. Kirchner, S. Lewandowski, E. Roeckl, and A. Sulik, GSI-Preprint-96-63 (1996), Nucl. Instr. Meth. B, in print.
- [3] J. Verplancke, E. Coenen, K. Cornelis, M. Huyse, G. Lhersonneau, and P. Van Duppen, *Z. Phys. A* 315 (1984) 307.
- [4] P. Decroock, Licentiaats Thesis, Leuven University, 1988, unpublished.
- [5] M. Huyse, P. del Marmol, E. Coenen, K. Deneffe, P. Van Duppen, and J. Vanhorenbeeck, *Z. Phys. A* 330 (1988) 121.

- [6] J. Szerypo, M. Huyse, G. Reusen, P. Van Duppen, Z. Janas, H. Keller, R. Kirchner, O. Klepper, A. Piechaczek, E. Roeckl, D. Schardt, K. Schmidt, R. Grzywacz, M. Pfützner, A. Plochocki, K. Rykaczewski, J. Żylicz, G. Alkhazov, L. Batist, A. Bykov, V. Wittmann, and B. A. Brown, *Nucl. Phys. A* 584 (1995) 221.
- [7] R. Kirchner, K. Burkard, W. Hüller, and O. Klepper, *Nucl. Instr. Meth.* 186 (1981) 295.
- [8] J. Szerypo, code SUMMING, 1996, to be published.
- [9] D. S. Andreev, K. I. Erokhina, V. S. Zvonov and I. Kh. Lemberg, *Izv. Akad. Nauk USSR, Ser. Fiz.* 37 (1973) 1609.
- [10] G. J. McCallum, and G. E. Coote, *Nucl. Instr. Meth.* 130 (1975) 189.
- [11] K. Debertin and R. G. Helmer, *Gamma- and X-ray spectrometry with semiconductor detectors* (North-Holland, Amsterdam, 1988) 258.
- [12] G. Lhersonneau, G. Dumont, K. Cornelis, M. Huyse, and J. Verplancke, *Phys. Rev. C* 18 (1978) 2688.
- [13] M. Palacz, J. Cederkäll, M. Lipoglavšek, J. Persson, A. Ataç, J. Blomqvist, H. Grawe, C. Fahlander, J. Iwanicki, A. Johnson, A. Kerek, J. Kownacki, A. Likar, L.-O. Norlin, J. Nyberg, R. Schubart, D. Seweryniak, Z. Sujkowski, R. Wyss, G. de Angelis, P. Bednarczyk, Zs. Dombrádi, D. Foltescu, D. Jerrestam, S. Juutinen, E. Mäkelä, G. Perez, M. de Poli, H. A. Roth, T. Shizuma, Ö. Skeppstedt, G. Sletten, S. Törmänen, and T. Vass, submitted to *Nucl. Phys. A* (1996).
- [14] G. Audi and A. H. Wapstra, *Nucl. Phys. A* 595 (1995) 409.
- [15] I.S. Towner, *Nucl. Phys. A* 444 (1985) 402.
- [16] D. de Frenne and E. Jacobs, *Nucl. Data Sheets* 68 (93) 935.
- [17] J. Blachot, *Nucl. Data Sheets* 62 (1991) 709.
- [18] S. Shastry, H. Bakhru, and I. M. Ladenbauer-Bellis, *Phys. Rev. C* 1 (1970) 1835.
- [19] L. Batist, V. Wittmann, G. Alkhazov, A. Bykov, H. Keller, R. Kirchner, E. Roeckl, P. Van Duppen, M. Huyse, G. Reuser, A. Plochocki, M. Pfützner, K. Rykaczewski, J. Szerypo, and J. Żylicz, in *GSI Sci. Rep. 1992*, GSI-Report 93-1 (1993) 82.
- [20] B. A. Brown and K. Rykaczewski, *Phys. Rev. C* 50 (1994) R2270.
- [21] *Table of Isotopes*, 8th Edn., eds. R. B. Firestone and V. S. Shirley. Wiley & Sons (New York, 1996).
- [22] S. A. Moszkowski, in *Alpha-, beta- and gamma-ray spectroscopy*, Vol. 2, ed. K. Siegbahn, North Holland (Amsterdam, 1974) 863.
- [23] F. Rösler, H. M. Fries, K. Alder and H. C. Pauli, *At. Data and Nucl. Data Tables* 21 (1978) 195.

Table 1

Energies, relative intensities and coincidence relations for  $\gamma$ -rays observed in the decay of  $^{103}\text{In}$  <sup>a</sup>

$\gamma$ -lines		Coincident $\gamma$ -lines
$E_\gamma$ [keV]	$I_\gamma^{rel}$	
156.7	0.35 (4)	
168.0	0.25 (3)	
177.8	0.54 (7)	
187.9	100	382, 538, 552, 573, 605, 720, 740, 754, 772, 872, 891, 917, 920, 947, 950, 995, 1089, 1145, 1159, 1179, 1181, 1327, 1411, 1426, 1474, 1591, 1666, 1677, 1690, 1732, 1784, 1887, 1915, 2007, 2212, 2386, 2425, 2453, 2585, 3305, 3383, 3642
190.8	0.03 (1)	
191.0	0.54 (9)	
202.0	17.8 (19)	157, 368, 391, 524, 538, 715, 871, 877, 899, 906, 1092, 1125, 1146, 1167, 1340, 1403, 1460, 1771, 2212
236.3 <sup>c</sup>	0.28 (3)	
265.3 <sup>c</sup>	1.12 (11)	
332.5 <sup>c</sup>	0.07 (1)	
334.0 <sup>c</sup>	0.26 (3)	
367.5	7.6 (8)	}157, 202, 535, 538, 740, 1402, 2212
367.7	0.77 (13)	
378.6	0.48 (11)	
381.7	0.51 (8)	
391.0	0.46 (8)	}178, 188, 202, 516, 525, 715, 977, 1581
391.7	5.6 (6)	
407.8	0.44 (7)	188
490.7	0.57 (10)	188, 202
515.6	0.19 (4)	
524.3	1.13 (12)	}202, 392
525.2	0.47 (8)	
535.1	0.47 (7)	
538.0	1.42 (29)	}188, 202, 368, 569, 754, 772, 1570
538.1	0.87 (11)	
538.3	0.92 (10)	
552.1	2.35 (26)	188, 191, 740, 772, 1040
569.4	4.48 (47)	157, 535, 538, 754, 1402, 2212
572.9	0.88 (10)	
586.7	1.03 (14)	
604.7	0.76 (10)	
648.5	0.24 (12)	
714.8	1.06 (14)	}202, 391
715.9	2.02 (28)	

$E_\gamma$ [keV]	$I_\gamma^{\text{rel}}$	Coincident $\gamma$ -lines
719.9	33.8 (36)	188, 573, 995, 1089, 1145, 1179, 1331, 1426, 1887, 1915, 1947, 2074
726.0	17.7 (19)	191, 379, 754, 872, 1019, 1064, 1570,
739.8	33.0 (35)	}168, 188, 368, 587, 649, 740, 772, 865, 1005 1040, 1050, 1086, 1180, 1188, 1232
740.4	2.22 (32)	
743.0 <sup>c</sup>	1.35 (23)	
754.4	4.4 (5)	538, 726
772.4	4.9 (5)	188, 649, 740
807.4 <sup>c</sup>	0.34 (4)	
864.3	0.18 (6)	
864.8	1.81 (22)	
871.0 <sup>b</sup>	0.35 (6)	}188, 202, 726
871.7	1.03 (14)	
877.0	0.49 (10)	
891.3	0.64 (13)	
892.3	0.96 (18)	
898.5 <sup>b</sup>	1.68 (21)	
905.7	1.21 (16)	
916.7	18.2 (19)	188, 191, 892, 1690
919.8	5.28 (56)	188, 864
946.6 <sup>b</sup>	0.64 (10)	
950.2 <sup>b</sup>	1.36 (17)	188
977.0	1.43 (17)	
994.8	2.37 (26)	188, 720
1005.0	1.50 (18)	
1018.5	1.51 (17)	188, 202, 726
1040.0	2.9 (3)	188, 740
1050.1	1.00 (14)	
1064.0	1.30 (23)	188
1085.9 <sup>b</sup>	1.43 (84)	
1089.1	1.60 (28)	
1092.0 <sup>b</sup>	0.82 (17)	
1107.3 <sup>b</sup>	7.3 (8)	
1124.7	1.41 (16)	
1145.0	2.10 (33)	
1145.6	0.43 (8)	
1159.3	1.30 (15)	
1167.1	1.01 (12)	
1178.6	1.72 (27)	188, 720, 740
1180.3	2.48 (37)	
1181.0	4.0 (6)	

$E_\gamma$ [keV]	$I_\gamma^{\text{rel}}$	Coincident $\gamma$ -lines
1188.1	1.73 (25)	
1219.5 <sup>c</sup>	0.50 (5)	
1232.0	1.34 (25)	188, 740
1292.6 <sup>c</sup>	0.41 (4)	
1326.8	4.80 (53)	188, 202
1331.1 <sup>b</sup>	2.20 (28)	188
1340.3 <sup>b</sup>	0.60 (10)	
1347.6 <sup>c</sup>	1.63 (18)	188
1368.5 <sup>c</sup>	1.81 (20)	
1397.8 <sup>c</sup>	1.07 (11)	
1402.3	0.62 (13)	} 368, 569
1402.6	0.73 (16)	
1410.5	4.1 (5)	188
1416.9 <sup>c</sup>	1.42 (15)	
1425.7	3.52 (43)	188, 720
1460.1	1.85 (24)	
1474.1	2.30 (26)	
1570.0	1.32 (25)	188, 726
1580.8	0.90 (14)	
1591.2 <sup>b</sup>	1.14 (16)	
1597.7 <sup>c</sup>	1.48 (15)	
1661.3 <sup>b</sup>	0.97 (12)	
1665.5 <sup>b</sup>	0.89 (13)	
1677.0 <sup>b</sup>	1.30 (16)	
1690.0	1.20 (25)	188, 917
1732.0	0.83 (13)	
1770.7 <sup>b</sup>	0.60 (13)	
1783.9	1.59 (19)	
1886.7	7.51 (84)	168, 188, 720
1915.2	4.45 (53)	188, 720
1943.1 <sup>c</sup>	0.48 (5)	
1947.0 <sup>b</sup>	1.46 (19)	
1972.0 <sup>c</sup>	5.1 (6)	
2007.2 <sup>b</sup>	1.52 (20)	
2054.5 <sup>c</sup>	0.78 (8)	
2073.6 <sup>b</sup>	0.53 (9)	
2082.6 <sup>c</sup>	0.83 (9)	
2089.8 <sup>b</sup>	1.27 (16)	
2211.7	3.87 (44)	188, 202, 368, 569
2347.0 <sup>c</sup>	1.03 (11)	
2386.3 <sup>b</sup>	2.27 (27)	188

$E_\gamma$ [keV]	$I_\gamma^{rel}$	Coincident $\gamma$ -lines
2424.5 <sup>b</sup>	1.16 (13)	
2452.8	2.56 (28)	188
2585.0	2.76 (29)	188
2605.6 <sup>c</sup>	0.38 (4)	
2899.7 <sup>c</sup>	0.53 (6)	
3001.9 <sup>b</sup>	0.93 (10)	
3087.8 <sup>c</sup>	1.42 (15)	
3256.4 <sup>c</sup>	1.01 (11)	
3305.0	3.43 (41)	188
3319.0 <sup>c</sup>	0.17 (2)	
3336.9 <sup>c</sup>	0.55 (6)	
3354.5 <sup>c</sup>	0.29 (3)	
3382.8	0.70 (9)	
3452.1 <sup>c</sup>	0.35 (4)	
3507.5 <sup>c</sup>	0.63 (7)	
3559.8 <sup>c</sup>	0.39 (4)	
3570.9 <sup>c</sup>	0.31 (4)	
3585.8 <sup>c</sup>	0.42 (4)	
3642.4	0.63 (8)	
3665.5 <sup>c</sup>	0.21 (2)	
3688.9 <sup>c</sup>	0.33 (3)	
3697.5 <sup>c</sup>	0.42 (4)	
3726.8 <sup>c</sup>	0.14 (1)	
3735.3 <sup>c</sup>	0.12 (1)	
3747.0 <sup>c</sup>	0.10 (1)	
3763.6 <sup>c</sup>	0.17 (2)	
3795.1 <sup>c</sup>	0.47 (5)	
3814.7 <sup>c</sup>	0.27 (3)	
3830.2 <sup>c</sup>	0.10 (1)	
3877.0 <sup>c</sup>	0.47 (5)	
3896.3 <sup>c</sup>	0.30 (3)	
3951.7 <sup>c</sup>	0.24 (3)	
3962.1 <sup>c</sup>	0.16 (2)	
3981.6 <sup>c</sup>	0.28 (3)	

<sup>a</sup> absolute intensities per 100 decays obtained by multiplying  $I_\gamma^{rel}$  by 0.485, the latter number being derived on the basis of  $\gamma$ -transitions placed in the decay scheme.

<sup>b</sup> placed tentatively in the decay scheme.

<sup>c</sup> not placed in the decay scheme.

Table 2

Shell-model predictions [20] for the integrated Gamow–Teller strengths  $B_{\Sigma}(\text{GT})$  and  $\beta$ -decay half-lives  $T_{1/2,\beta}$  of ground state and isomer of  $^{99}\text{In}$  and  $^{101}\text{In}$ . The predictions take a Gamow–Teller quenching factor of 7.0 into account (see text). The excitation energies  $E^*$  of the isomers result also from the shell-model calculations

Nuclide	$E^*$ (keV)	$B_{\Sigma}(\text{GT})$	$T_{1/2,\beta}$ (s)
$^{99g}\text{In}$	0	2.3	2.1
$^{99m}\text{In}$	386	2.5	2.3
$^{101g}\text{In}$	0	2.0	13
$^{101m}\text{In}$	500	2.1	19

Table 3

Data on  $\beta$ -decay branching ratios for M4 isomers in odd-A indium isotopes.  $T_{1/2,\gamma+ce}^M$  is the Moszkowski single-proton estimate [22], including the total M4 internal conversion coefficient [23],  $T_{1/2,\gamma+ce}^{\text{scaled}}$  for  $^{101m}\text{In}$ ,  $^{103m}\text{In}$  and  $^{105m}\text{In}$  is obtained by scaling  $T_{1/2,\gamma+ce}^M$  with the ratio limits  $T_{1/2,\gamma+ce}^M/T_{1/2}^{\text{exp}}$  derived for  $^{107m}\text{In}$  and  $^{109m}\text{In}$ . On the basis of a comparison of  $T_{1/2,g.s.}^{\text{exp}}$  and  $T_{1/2}^{\text{exp}}$ , it is assumed that  $I_{\beta}=0$  for  $^{107m}\text{In}$  and  $^{109m}\text{In}$

Nuclide	$T_{1/2,g.s.}^{\text{exp}}$	$E_{\gamma}$ (keV)	$T_{1/2}^{\text{exp}}$ (s)	$T_{1/2,\gamma+ce}^M$ (s)	$T_{1/2,\gamma+ce}^{\text{scaled}}$ (s)	$T_{1/2,\beta}$ (s)	$I_{\gamma+ce}$ (%)	$I_{\beta}$ (%)
$^{109m}\text{In}$	4.2(1) h	650.1	80.4(42)	54.8	80.4	$\infty$	100	0
$^{107m}\text{In}$	32.4(3) min	678.5	50.4(6)	39.1	50.4	$\infty$	100	0
$^{105m}\text{In}$	5.07(7) min	674.1	48(6)	43.0	55–63	192–135	68.1–77.6	31.9–22.4
$^{103m}\text{In}$	60(1) s <sup>a</sup>	631.7 <sup>a</sup>	34(2) <sup>a</sup>	78.8	102–116	51–48	29.4–33.4	70.6–66.6
$^{101m}\text{In}$	14.9(12) s <sup>a</sup>	$\sim 600^b$	$<15^c$	128	165–188	$<16.5$	$<9$	$>91$

<sup>a</sup> Result from this work; previously obtained value of  $T_{1/2,g.s.}^{\text{exp}}$  for  $^{101m}\text{In}$ : 16(3) s [5].

<sup>b</sup> No experimental value known; 600 keV taken as a rough estimate based on experimental systematics.

<sup>c</sup> No experimental value known: ground state half-life assumed as an upper limit.



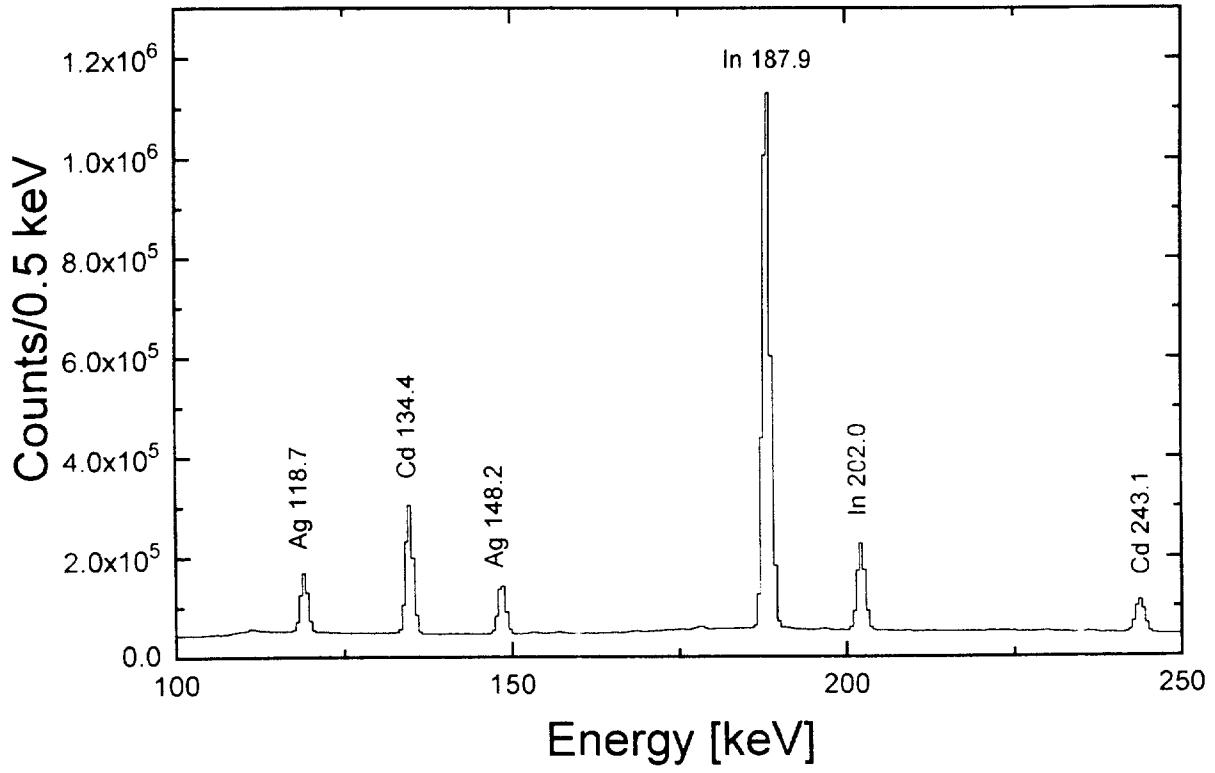


Fig. 1

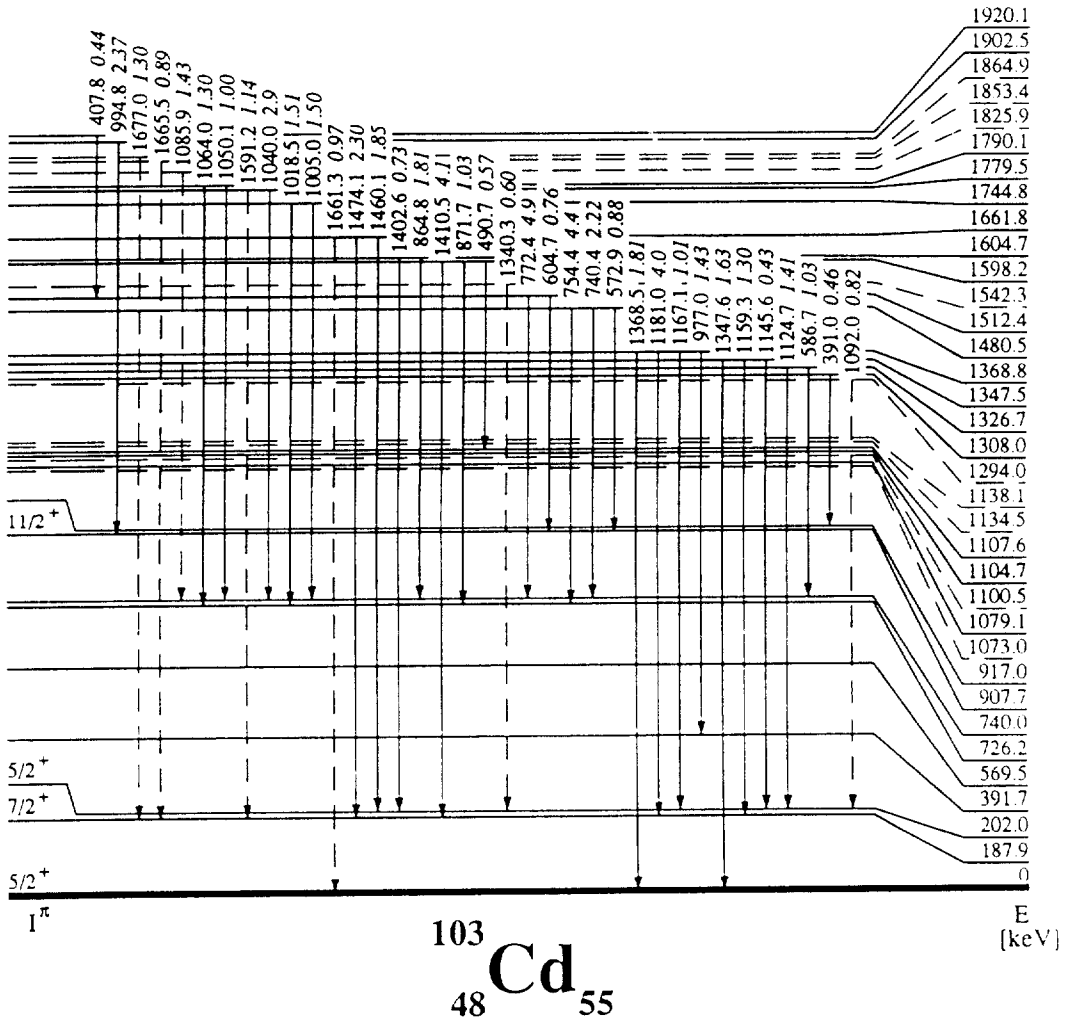
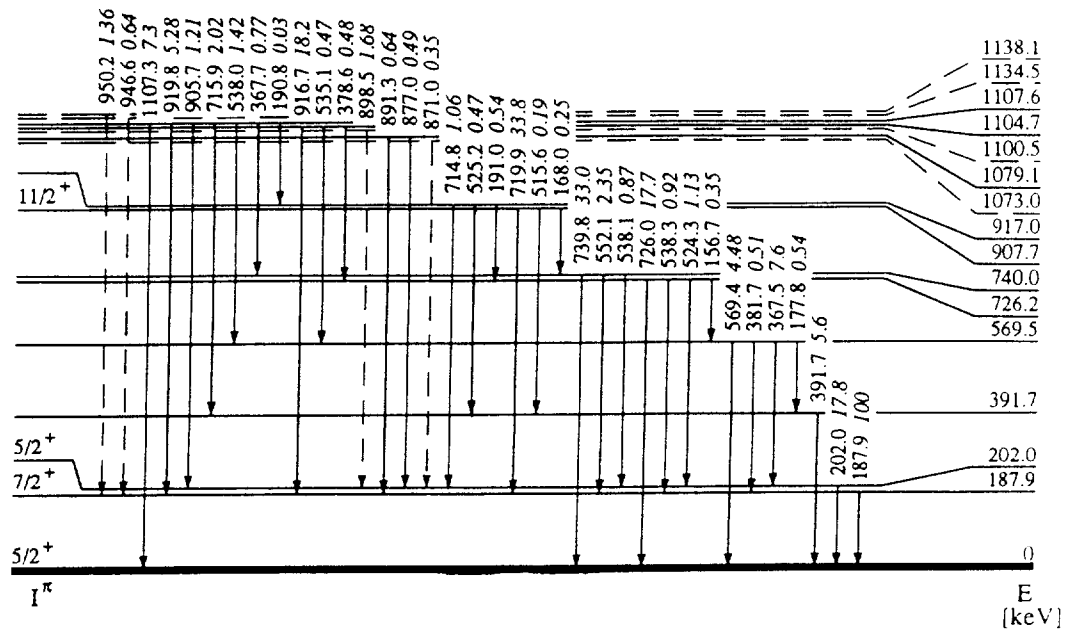


Fig. 2 (part 1)

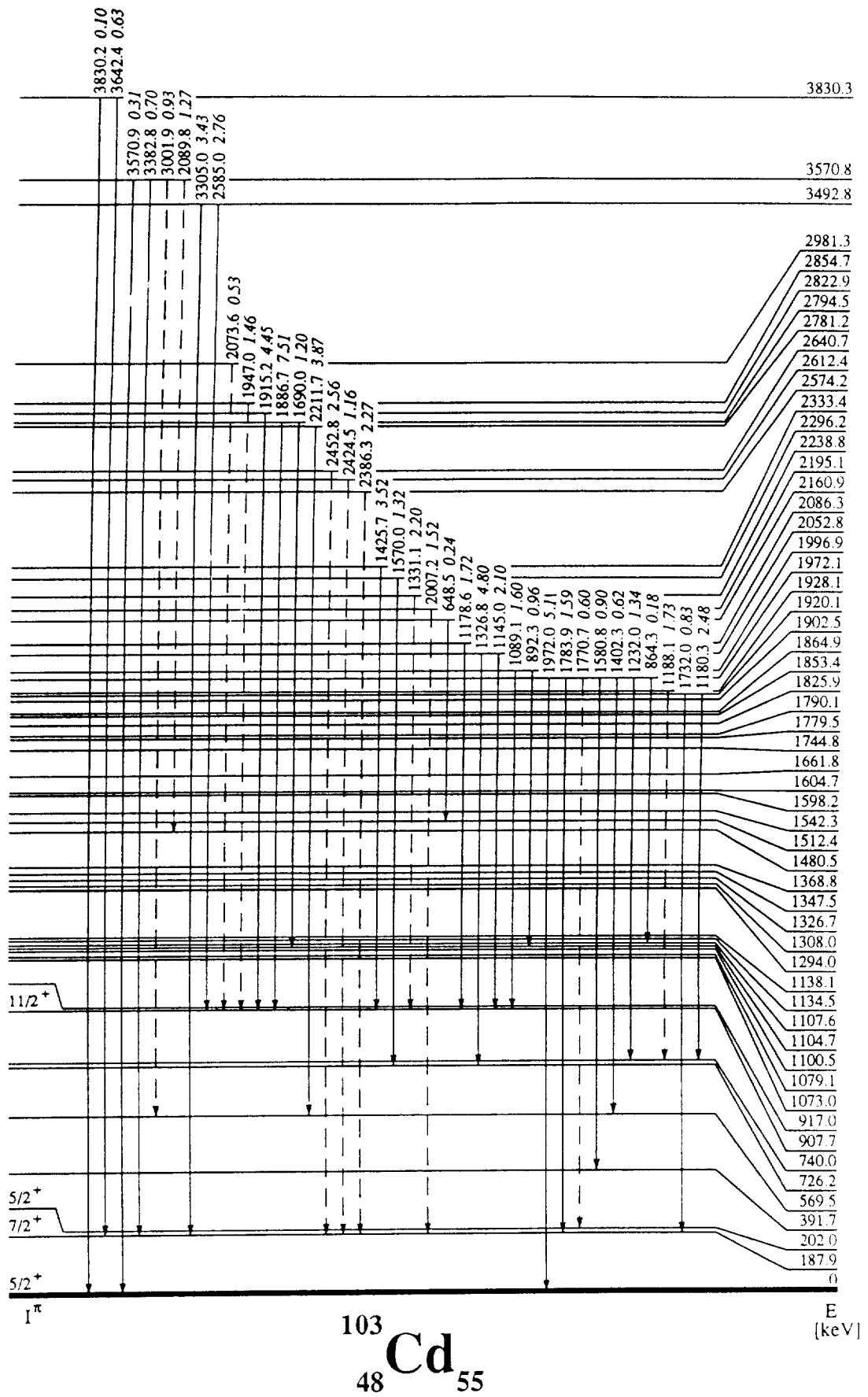


Fig. 2 (part 2)

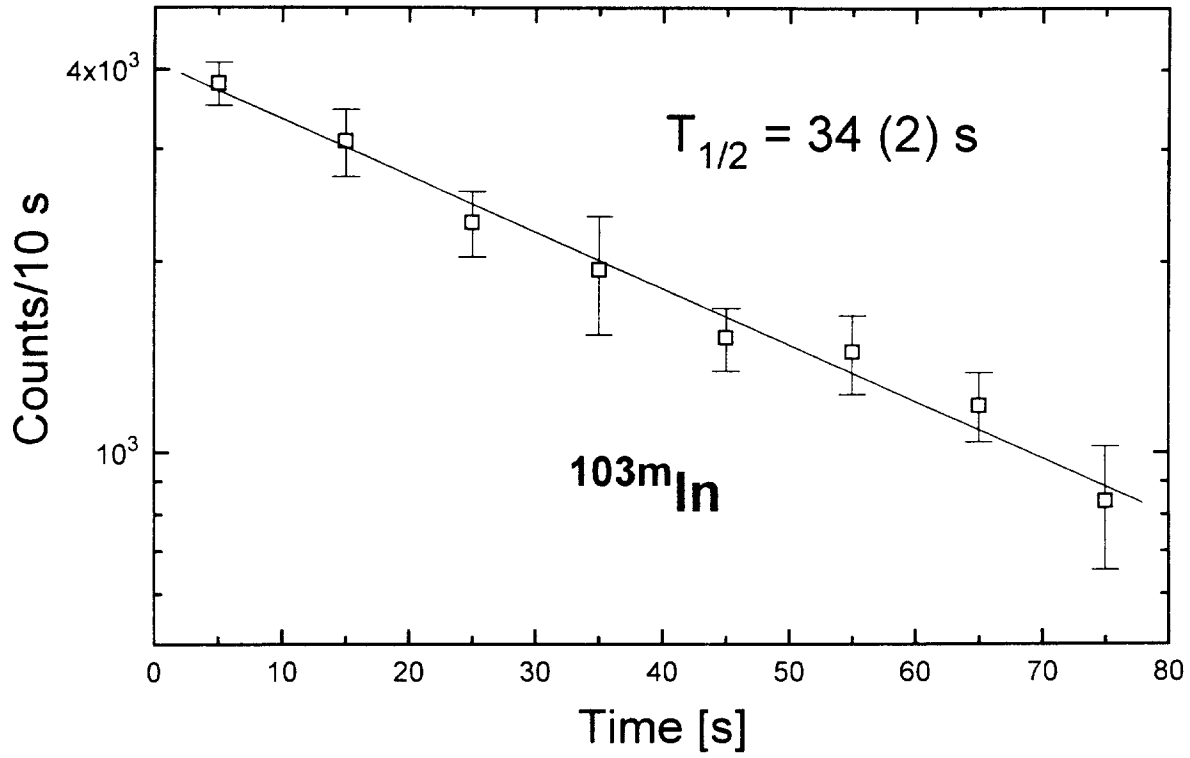


Fig. 3

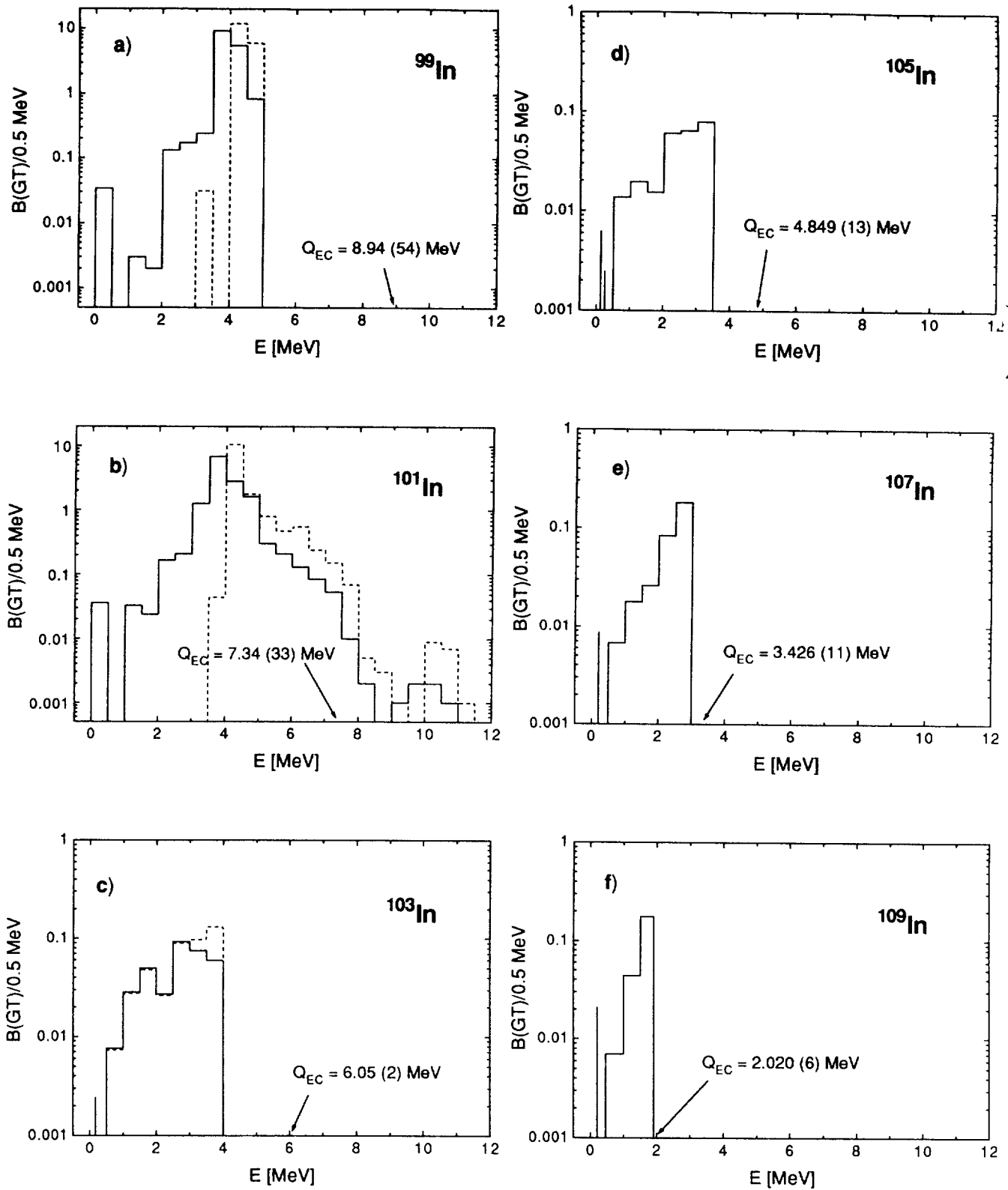


Fig. 4